Acta Cryst. (1996). B52, 746–752

Tautomerism in 3{5}-(Dimethoxyphenyl)pyrazoles

MALCOLM A. HALCROW,* HAROLD R. POWELL AND MELINDA J. DUER

Department of Chemistry, University of Cambridge, Lensfield Road, Cambridge CB2 1EW, England. E-mail: mah26@cam.ac.uk

(*Received 28 February 1996; accepted 22 April 1996*)

Abstract

The single crystal X-ray structures of 3{5}-(2′,5′-dimethoxyphenyl)pyrazole (III) and the hemihydrate of 3{5}-(3′,4′-dimethoxyphenyl)pyrazole (IV) have been determined. Compound (III) exists purely as the 5-substituted prototropomer in the crystal; the pyrazole pyrollic N—H proton is involved in a three-way hydrogen bond, involving an intramolecular contact with a methoxy oxygen donor and an intermolecular interaction to the pyridinic N atom of a neighbouring molecule, forming discrete hydrogen-bonded dimers. There is no evidence of degenerate proton transfer within the dimeric units from CPMAS ^{13}C NMR spectroscopy, in contrast to other known pyrazoles that associate in this manner. In (IV).1/2H_2O, however, the pyrrolic proton is disordered over both N(1) and N(2) *via* hydrogen bonding to the solvate water molecule. CPMAS ^{13}C NMR spectroscopy shows that the prototropic disorder in (IV).1/2H_2O is static at temperatures up to 370 K. Solution ^{1}H and ^{13}C NMR data in DMSO-d_6 show that for both (III) and (IV) the 3- and 5-substituted tautomeric forms are similarly populated in this solvent, suggesting both that the intramolecular hydrogen bond in (III) has been disrupted and that the two tautomers of (III) and (IV) are close in energy.

1. Introduction

There is continuing interest in the structural chemistry and prototropy of C-substituted pyrazoles. The pyrazole ring, which contains both a proton-donor pyrrolic N—H group and proton-acceptor pyridinic N atom in adjacent positions, affords a complex physical chemistry for these molecules in the gas, solution and solid phases (Abboud *et al.*, 1992; Llamas-Saiz, Foces-Foces & Elguero, 1994; Llamas-Saiz *et al.*, 1994). This bifunctionality also often affords unusual crystal packing arrangements for 3{5}-substituted pyrazoles *via* intermolecular hydrogen bonding, which can give rise to complex fluxionality in the solid state involving degenerate intermolecular proton transfer reactions, which may be coupled with other molecular motions and can be sensitively probed by ^{1}H, ^{13}C and ^{15}N NMR spectroscopies (Smith *et al.*, 1989; Aguilar-Parrilla, Cativiela *et al.*, 1992; Aguilar-Parrilla, Scherer *et al.*, 1992; Llamas-Saiz, Foces-Foces, Elguero & Meutermans, 1992; Llamas-Saiz, Foces-Foces, Sobrados, Elguero & Meutermans, 1993; Foces-Foces, Llamas-Saiz, Claramunt, López & Elguero, 1994; Elguero *et al.*, 1994; Aguilar-Parrilla *et al.*, 1995). Several 3{5}-(2′-hydroxyaryl)pyrazoles are also good UV stabilizers, a property that is linked to the presence of an intramolecular N···H—O hydrogen bond in these compounds which facilitates intramolecular proton transfer upon excitation (Catalán *et al.*, 1992). The prototype for the above proton transfer processes is the tautomeric equilibrium shown in Fig. 1, whose rate in solution can vary drastically in different solvents and whose position depends on both the identity of the pyrazole substituents and on the phase of matter examined; there are at least two reports of pyrazoles favouring different prototropomers in solution and the solid state (Aguilar-Parrilla, Cativiela *et al.*, 1992; Lopez, Claramunt, Trofimenko & Elguero, 1993).

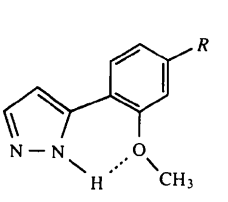

(I): R = H
(II): R = OMe

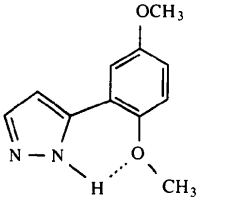

(III)

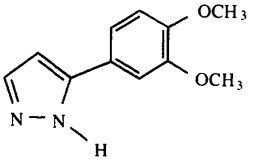

(IV)

A recent solution and solid-state ^{13}C NMR study of 29 different N—H pyrazoles concluded that the preferred position of the pyrazole acidic proton (*i.e.* the position of the equilibrium in Fig. 1) could be correlated with the Hammett σ_m parameter of the 3{5}-substituent, substituents with positive σ_m values prefer the 3-position while those with negative σ_m adopt the 5-position (Lopez, Claramunt, Trofimenko &

Elguero, 1993). However, the two (methoxyphenyl)-substituted pyrazoles (I) and (II) examined in this work did not follow this trend, showing ^{13}C spectra consistent with a 5-substituted isomer in the solid state and solution, despite the general preference for the 3-position shown by other 3{5}-aryl pyrazoles, including a 3{5}-trimethoxyphenyl derivative (Cativiela, Laureiro, Elguero & Elguero, 1991; Aguilar-Parrilla, Cativiela *et al.*, 1992; Lopez, Claramunt, Trofimenko & Elguero, 1993). The authors attributed this anomaly to the presence of intramolecular hydrogen bonds in (I) and (II) between the 2-methoxy donor and pyrazole N—H group, although no structural data was presented to corroborate this assumption.

As part of our program to examine the coordination chemistry of hydroquinone-containing ligands, we have recently synthesized two structural isomers of (II), namely 3{5}-(2′,5′-dimethoxyphenyl)pyrazole (III) and 3{5}-(3′,4′-dimethoxyphenyl)pyrazole (IV), as precursors for polydentate ligands to transition metals (Halcrow, Cromhout, Powell & Raithby, 1996; Halcrow, Raithby & Rennie, 1996). We report here the single crystal structures of (III) and the hemihydrate of (IV), together with solid-state and solution NMR data that facilitate the discussion of tautomerism in these compounds.

2. Experimental

Compounds (III) and (IV) were prepared from the corresponding dimethoxyacetophenones according to the method of Lin & Lang [1977 (Halcrow, Cromhout, Powell & Raithby, 1996)]. Layering of chloroform solutions of both compounds with hexanes afforded large colourless blocks. Crystals of (IV) grown by this method analyse as the hemihydrate (calc. for $C_{11}H_{12}N_2O_2.1/2H_2O$: C 62.0, H 6.14, N 13.1; found: C 61.9, H 6.07, N 13.2), a proposition confirmed by the subsequent structure determination, while those of (III) are solvent-free (calc. for $C_{11}H_{12}N_2O_2$: C 64.7, H 5.92, N 13.7; found: C 64.7, H 5.88, N 13.9).

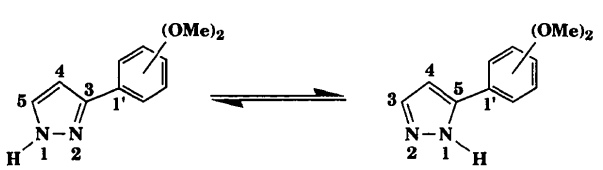

A 3-substituted *B* 5-substituted

Fig. 1. Tautomeric equilibria for 3{5}-substituted pyrazoles, with the different atom numbering conventions employed for the two prototropomers.

2.1. *X-ray structure determinations*

Details of the crystal data, data collection and structure refinements are given in Table 1. The structures were solved by direct methods (*SHELXTL-Plus*; Sheldrick, 1987) and refined using full-matrix least-squares analysis on F^2 (*SHELXL*93; Sheldrick, 1993). In both structures all non-H atoms were refined anisotropically and all carbon-bound H atoms were refined in fixed calculated positions with calculated thermal parameters. For (III) the pyrrolic H(1) atom was refined in a calculated position exclusively bonded to N(1). The structure of (IV).1/2H_2O was initially refined in the same way; however, following examination of the packing diagram and NMR data for this compound, the N—H proton was rerefined in calculated positions as two half-occupied H(1) and H(2) atoms bound to N(1) and N(2), respectively. Similarly, the water proton in (IV).1/2H_2O was modelled over two half-occupied orientations [H(1*WA*) and H(1*WB*)], which were restrained to a fixed O—H distance of 0.96 (3) Å and H—O—H angle of 109 (3)°.*

2.2. *Spectroscopic studies*

Solution NMR spectra were obtained using a Bruker AC250 spectrometer operating at 250.1 and 62.9 MHz for ^1H and ^{13}C, respectively. CPMAS ^{13}C NMR spectra were recorded with a Chemagnetics CMX400 spectrometer operating at 399.9 (^1H) and 100.6 MHz (^{13}C), using a standard cross-polarization pulse sequence with a 90° pulse of 4.95μs, contact time 10 ms and recycle delay 10 s. Spectra at different spinning speeds were recorded and compared to identify spinning side-bands.

3. Results and discussion

The molecular structures of (III) and (IV) are shown in Figs. 2 and 3, while bond lengths and angles for these compounds are listed in Tables 4 and 5. The internal bond lengths and angles for both molecules are unexceptional and will not be discussed further.

As previously proposed for (I) and (II) (Lopez, Claramunt, Trofimenko & Elguero, 1993), there is an intramolecular hydrogen bond between the pyrazole N—H group and the 2′-methoxy O-donor in the structure of (III), with N(1)—O(11) 2.641 (2) Å, N(1)—H(1)—O(11) 121.8° (Fig. 2). As a result of this hydrogen bond, the planes of the pyrazole and aryl rings are only slightly twisted, the dihedral angle between them being 15.47 (11)°. This is the first crystallographically characterized intramolecular

* Lists of atomic coordinates, anisotropic displacement parameters and structure factors have been deposited with the IUCr (Reference: BM0005). Copies may be obtained through The Managing Editor, International Union of Crystallography, 5 Abbey Square, Chester CH1 2HU, England.

Table 1. *Experimental details*

	(III)	(IV)
Crystal data		
Chemical formula	$C_{11}H_{12}N_2O_2$	$C_{11}H_{12}N_2O_2.0.5H_2O$
Chemical formula weight	204.23	213.23
Cell setting	Monoclinic	Monoclinic
Space group	$P2_1/c$	$C2/c$
a (Å)	11.376 (2)	30.524 (3)
b (Å)	6.4421 (8)	8.9917 (12)
c (Å)	14.419 (3)	8.1542 (9)
β (°)	90.01 (2)	101.057 (8)
V (Å^3)	1056.8 (3)	2196.5 (4)
Z	4	8
D_x (Mg m^{-3})	1.284	1.290
Radiation type	Cu $K\alpha$	Cu $K\alpha$
Wavelength (Å)	1.54178	1.54178
No. of reflections for cell parameters	25	25
θ range (°)	59.2–60.0	59.5–60.0
μ (mm^{-1})	0.738	0.766
Temperature (K)	293 (2)	293 (2)
Crystal form	Block	Barrel
Crystal size (mm)	0.36 × 0.22 × 0.18	0.45 × 0.45 × 0.20
Crystal colour	Colourless	Colourless
Data collection		
Diffractometer	Rigaku AFC-7*R*	Rigaku AFC-7*R*
Data collection method	ω–2θ scans	ω–2θ scans
Absorption correction	ψ scans (*XEMP*; Sheldrick, 1987)	ψ scans (*XEMP*; Sheldrick, 1987)
T_{min}	0.904	0.893
T_{max}	0.998	0.999
No. of measured reflections	3130	2315
No. of independent reflections	1571	1635
No. of observed reflections	1444	1455
Criterion for observed reflections	$I > 2\sigma(I)$	$I > 2\sigma(I)$
R_{int}	0.0482	0.0111
θ_{max} (°)	60.15	60.16
Range of h, k, l	$-12 \rightarrow h \rightarrow 1$ $-7 \rightarrow k \rightarrow 1$ $-16 \rightarrow l \rightarrow 16$	$-34 \rightarrow h \rightarrow 34$ $-1 \rightarrow k \rightarrow 10$ $-1 \rightarrow l \rightarrow 9$
No. of standard reflections	3	3
Frequency of standard reflections	Every 100 reflections	Every 100 reflections
Intensity decay (%)	0.44	2.7
Refinement		
Refinement on	F^2	F^2
$R[F^2 > 2\sigma(F^2)]$*	0.0372	0.0377
$wR(F^2)$†	0.1588	0.1121
S	0.872	0.893
No. of reflections used in refinement	1571	1635
No. of parameters used	137	147
H-atom treatment	H atoms placed in calculated positions	H atoms placed in calculated positions
Weighting scheme	$w = 1/[\sigma^2(F_o^2) + (0.1608P)^2 + 0.0311P]$, where $P = (F_o^2 + 2F_c^2)/3$	$w = 1/[\sigma^2(F_o^2) + (0.0764P)^2 + 1.4885P]$, where $P = (F_o^2 + 2F_c^2)/3$
$(\Delta/\sigma)_{max}$	−0.015	0.0
$\Delta\rho_{max}$ (e Å^{-3})	0.158	0.140
$\Delta\rho_{min}$ (e Å^{-3})	−0.166	−0.172
Extinction method	*SHELXL*93 (Sheldrick, 1993)	None
Extinction coefficient	0.0216 (32)	–
Source of atomic scattering factors	*International Tables for Crystallography* (1992, Vol. C, Tables 4.2.6.8 and 6.1.1.4)	*International Tables for Crystallography* (1992, Vol. C, Tables 4.2.6.8 and 6.1.1.4)
Computer programs		
Structure solution	*SHELXS*86 (Sheldrick, 1990)	*SHELXS*86 (Sheldrick, 1990)
Structure refinement	*SHELXL*93 (Sheldrick, 1993)	*SHELXL*93 (Sheldrick, 1993)
Preparation of material for publication	*XP* (Sheldrick, 1987)	*XP* (Sheldrick, 1987)

* $R = \Sigma[|F_o| - |F_c|]/\Sigma|F_o|$. † $wR = [\Sigma w(F_o^2 - F_c^2)/\Sigma wF_o^4]^{1/2}$.

N{pyrrolic}—H···O hydrogen bond within a substituted pyrazole, although a related N{pyridinyl}···H—O interaction is present in the solid-state structure of 5-(2′-hydroxyphenyl)pyrazole (Catalán *et al.*, 1992). Interestingly, H(1) is also involved in an intermolecular hydrogen bond with N(2) of a neighbouring molecule with N(1)—N(2′) 2.950 (2) Å, N(1)—H(1)—N(2′) 136.9°, forming a cyclic dimer (Fig. 2); this mode of intermolecular association is also present in the published crystal structures of 3,5-di(*tert*-butyl)- and

Table 2. *Fractional atomic coordinates and equivalent isotropic displacement parameters (Å²) for (III)*

$U_{eq} = (1/3)\Sigma_i\Sigma_j U_{ij} a_i^* a_j^* \mathbf{a}_i.\mathbf{a}_j.$

	x	y	z	U_{eq}
N(1)	0.87856 (11)	0.0161 (2)	0.44422 (8)	0.0492 (4)
N(2)	0.88693 (11)	0.1552 (2)	0.51353 (8)	0.0554 (5)
C(3)	0.78953 (14)	0.2652 (3)	0.50582 (11)	0.0573 (5)
C(4)	0.72014 (13)	0.1998 (3)	0.43314 (11)	0.0555 (5)
C(5)	0.78050 (11)	0.0369 (2)	0.39307 (9)	0.0449 (5)
C(1′)	0.75336 (11)	−0.0846 (2)	0.30959 (10)	0.0441 (4)
C(2′)	0.81281 (12)	−0.2681 (2)	0.28686 (11)	0.0488 (5)
C(3′)	0.78465 (14)	−0.3725 (3)	0.20577 (12)	0.0582 (5)
C(4′)	0.69931 (15)	−0.2984 (3)	0.14739 (11)	0.0589 (5)
C(5′)	0.63946 (13)	−0.1168 (2)	0.16863 (10)	0.0503 (5)
C(6′)	0.66711 (12)	−0.0115 (2)	0.24916 (10)	0.0475 (5)
O(11)	0.89773 (9)	−0.3306 (2)	0.34770 (9)	0.0618 (4)
C(12)	0.9675 (2)	−0.5057 (3)	0.32532 (15)	0.0705 (6)
O(13)	0.55723 (10)	−0.0533 (2)	0.10512 (8)	0.0639 (4)
C(14)	0.4945 (2)	0.1314 (3)	0.12400 (12)	0.0680 (6)

Table 3. *Fractional atomic coordinates and equivalent isotropic displacement parameters (Å²) for (IV)*

$U_{eq} = (1/3)\Sigma_i\Sigma_j U_{ij} a_i^* a_j^* \mathbf{a}_i.\mathbf{a}_j.$

	x	y	z	U_{eq}
N(1)	0.44712 (5)	0.1888 (2)	0.3306 (2)	0.0514 (4)
N(2)	0.46545 (5)	0.2393 (2)	0.4837 (2)	0.0588 (4)
C(3)	0.44806 (7)	0.3726 (2)	0.5008 (2)	0.0595 (5)
C(4)	0.41835 (6)	0.4086 (2)	0.3578 (2)	0.0548 (5)
C(5)	0.41836 (5)	0.2896 (2)	0.2507 (2)	0.0429 (4)
C(1′)	0.39279 (5)	0.2651 (2)	0.0816 (2)	0.0419 (4)
C(2′)	0.35011 (5)	0.3275 (2)	0.0365 (2)	0.0456 (4)
C(3′)	0.32546 (5)	0.3094 (2)	−0.1217 (2)	0.0457 (4)
C4(′)	0.34303 (5)	0.2272 (2)	−0.2409 (2)	0.0443 (4)
C5(′)	0.38483 (6)	0.1652 (2)	−0.1963 (2)	0.0492 (4)
C(6′)	0.40951 (6)	0.1844 (2)	−0.0367 (2)	0.0490 (4)
O(11)	0.28394 (4)	0.3664 (2)	−0.1771 (2)	0.0666 (4)
C(12)	0.26547 (7)	0.4562 (3)	−0.0645 (3)	0.0907 (8)
O(13)	0.31603 (4)	0.21673 (14)	−0.39409 (14)	0.0580 (4)
C(14)	0.33208 (7)	0.1350 (3)	−0.5195 (2)	0.0716 (6)
O(1*W*)	1/2	−0.0493 (2)	1/4	0.0471 (4)

Table 4. *Selected geometric parameters (Å, °) for (III)*

N(1)—C(5)	1.344 (2)	C(2′)—O(11)	1.365 (2)
N(1)—N(2)	1.346 (2)	C(2′)—C(3′)	1.386 (2)
N(2)—C(3)	1.320 (2)	C(3′)—C(4′)	1.371 (2)
C(3)—C(4)	1.378 (2)	C(4′)—C(5′)	1.388 (2)
C(4)—C(5)	1.381 (2)	C(5′)—O(13)	1.372 (2)
C(5)—C(1′)	1.469 (2)	C(5′)—C(6′)	1.381 (2)
C(1′)—C(6′)	1.394 (2)	O(11)—C(12)	1.416 (2)
C(1′)—C(2′)	1.401 (2)	O(13)—C(14)	1.413 (2)
C(5)—N(1)—N(2)	113.57 (11)	O(11)—C(2′)—C(1′)	116.10 (13)
C(3)—N(2)—N(1)	103.63 (12)	C(3′)—C(2′)—C(1′)	119.69 (14)
N(2)—C(3)—C(4)	112.37 (13)	C(4′)—C(3′)—C(2′)	120.83 (15)
C(3)—C(4)—C(5)	105.42 (13)	C(3′)—C(4′)—C(5′)	120.37 (14)
N(1)—C(5)—C(4)	105.00 (12)	O(13)—C(5′)—C(6′)	124.76 (14)
N(1)—C(5)—C(1′)	124.83 (12)	O(13)—C(5′)—C(4′)	116.03 (13)
C(4)—C(5)—C(1′)	130.05 (13)	C(6′)—C(5′)—C(4′)	119.20 (15)
C(6′)—C(1′)—C(2′)	118.58 (13)	C(5′)—C(6′)—C(1′)	121.33 (14)
C(6′)—C(1′)—C(5)	118.71 (13)	C(2′)—O(11)—C(12)	118.99 (14)
C(2′)—C(1′)—C(5)	122.69 (13)	C(5′)—O(13)—C(14)	117.81 (12)
O(11)—C(2′)—C(3′)	124.20 (14)		

Table 5. *Selected geometric parameters (Å, °) for (IV)*

N(1)—C(5)	1.340 (2)	C(2′)—C(3′)	1.372 (2)
N(1)—N(2)	1.345 (2)	C(3′)—O(11)	1.361 (2)
N(2)—C(3)	1.330 (2)	C(3′)—C(4′)	1.407 (2)
C(3)—C(4)	1.372 (2)	C(4′)—O(13)	1.361 (2)
C(4)—C(5)	1.381 (2)	C(4′)—C(5′)	1.376 (2)
C(5)—C(1′)	1.465 (2)	C(5′)—C(6′)	1.384 (2)
C(1′)—C(6′)	1.381 (2)	O(11)—C(12)	1.419 (2)
C(1′)—C(2′)	1.402 (2)	O(13)—C(14)	1.421 (2)
C(5)—N(1)—N(2)	109.90 (14)	O(11)—C(3′)—C(2′)	125.13 (15)
C(3)—N(2)—N(1)	107.34 (14)	O(11)—C(3′)—C(4′)	114.96 (14)
N(2)—C(3)—C(4)	109.6 (2)	C(2′)—C(3′)—C(4′)	119.91 (14)
C(3)—C(4)—C(5)	105.9 (2)	O(13)—C(4′)—C(5′)	125.60 (15)
N(1)—C(5)—C(4)	107.22 (14)	O(13)—C(4′)—C(3′)	115.24 (14)
N(1)—C(5)—C(1′)	122.48 (14)	C(5′)—C(4′)—C(3′)	119.16 (15)
C(4)—C(5)—C(1′)	130.29 (14)	C(4′)—C(5′)—C(6′)	120.5 (2)
C(6′)—C(1′)—C(2′)	118.45 (15)	C(1′)—C(6′)—C(5′)	121.01 (15)
C(6′)—C(1′)—C(5)	122.36 (14)	C(3′)—O(11)—C(12)	117.33 (14)
C(2′)—C(1′)—C(5)	119.19 (14)	C(4′)—O(13)—C(14)	117.70 (14)
C(3′)—C(2′)—C(1′)	120.92 (15)		

3,5-diphenylpyrazole (Aguilar-Parilla, Scherer *et al.*, 1992; Llamas-Saiz *et al.*, 1994; Aguilar-Parilla *et al.*, 1995). These dimers are stacked so as to form diagonal columns which lie perpendicular to each other in the lattice, although not in a manner permitting graphitic interactions between molecules.

The asymmetric unit of (IV).1/2H_2O contains one molecule of pyrazole in a general position (Fig. 3), which is hydrogen bonded to a molecule of water lying on the crystallographic twofold axis, with N(1)—O(1*W*) 2.834 (2) Å, N(1)—H(1)—O(1*W*) 148.7°. The water

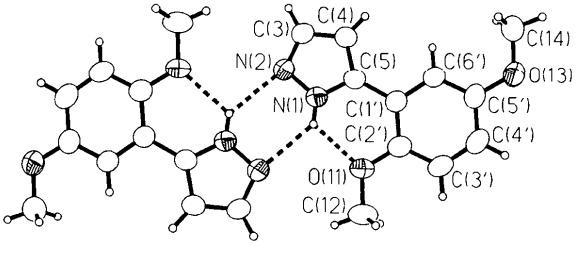

Fig. 2. The molecular structure of (III), showing the atom numbering scheme employed and the arrangement of molecules of (III) into intermolecularly hydrogen-bonded dimers. Thermal ellipsoids are drawn at the 50% probability level, except those for H which have arbitrary radii.

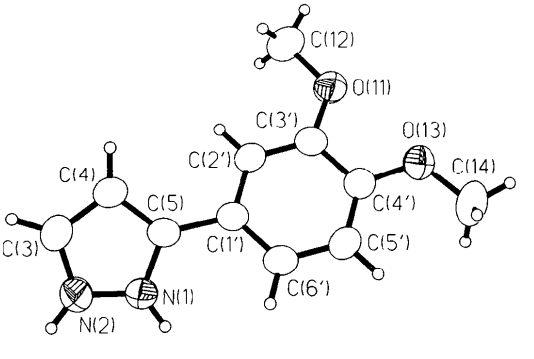

Fig. 3. The molecular structure of (IV), showing the atom numbering scheme employed. Thermal ellipsoids are drawn at the 50% probability level, except those for H which have arbitrary radii. Both orientations of the disordered pyrrolic proton [H(1) and H(2)] are shown.

solvate is in turn hydrogen bonded to the pyridyl N atom of a pyrazole molecule in a neighbouring asymmetric unit, with N(2′)—O(1*W*) 2.805 (2) Å, N(2′)—H(1*WB*)—O(1*W*) 175.6° (Figs. 4 and 5). This arrangement of two donor and two acceptor hydrogen bonds to the central water molecule allows for disorder of the pyrazole N—H and water protons, and implies that the pyrazole N—H H atoms should be disordered between the N(1) and N(2) sites (Figs. 3 and 5); the pyrazole N—H H(1) and H(2) atoms, and the two orientations of the water proton H(1*WA*) and H(1*WB*), were successfully refined with 50% occupancy assuming this disorder, the alternative disorder orientation containing H(2) and H(1*WA*) yielding intermolecular hydrogen bonds with N(2)—H(2)—O(1*W*) 150.5° and N(1′)—H(1*WA*)—O(1*W*) 164.2°. There is a dihedral angle of 148.22 (9)° between the planes of the pyrazole and dimethoxyphenyl groups, demonstrating the expected free rotation between the two unsaturated rings.

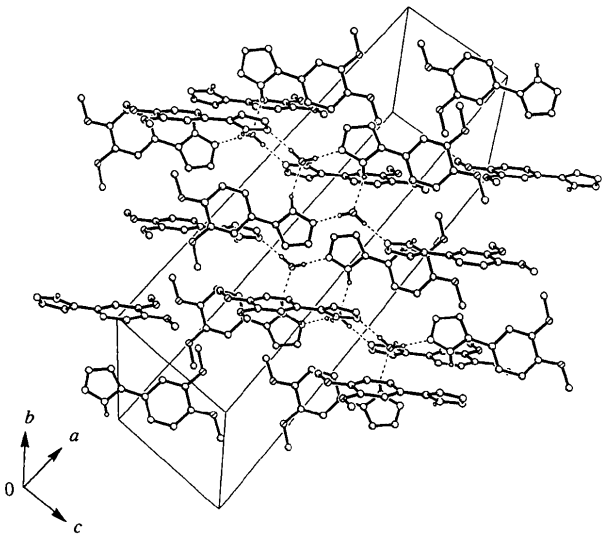

Fig. 4. Packing diagram for (IV).1/2H_2O. For clarity, all H atoms except H(1) and H(1*WB*) have been omitted, while only one orientation of the prototropic disorder is shown.

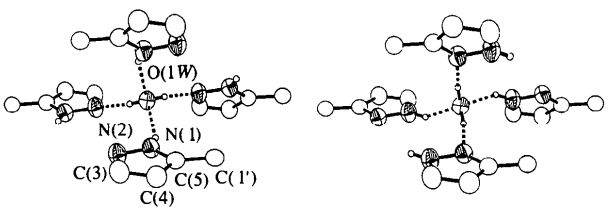

Fig. 5. The environment about the solvate water molecule in (IV).1/2H_2O, showing the two disorder orientations for the pyrazole N—H and water H atoms. For clarity, only the *ipso*-C atoms [C(1′)] of the dimethoxyphenyl substituents are shown, while all carbon-bound H atoms have been omitted. Atom O(1*W*) lies on a site of crystallographic 2_1 symmetry.

The refinement of (III) as an ordered structure containing exclusively the 5-substituted isomer is supported by the structural dimensions within the pyrazole unit. Previous surveys of the molecular geometries of pyrazoles have employed as structural indices the differences in N—N—C angles {ΔN (°) = [N(2)—N(1)—C(5)] − [N(1)—N(2)—C(3)]} and the difference in C—N distances {Δr_{CN} (Å) = [N(1)—C(5)] − [N(2)—C(3)]} within the pyrazole ring (Bonati, 1989; Llamas-Saiz, Foces-Foces & Elguero, 1994). For (III), ΔN = 9.9° and $10^2\Delta r_{CN}$ = 2.4 Å, which lie within the normal ranges for *N*-unsubstituted pyrazoles of ΔN = 7.0–11.3° and $10^2\Delta r_{CN}$ = − 0.1 to 4.6 Å and so are consistent with an ordered molecular structure. By contrast, these indices for (IV).1/2H_2O are ΔN = 2.6° and $10^2\Delta r_{CN}$ = 1.0 Å, and are incompatible with an ordered structure for this molecule.

The observation of *both* tautomers *A* and *B* (Fig. 1) in the crystal structure of (IV).1/2H_2O is unique for an asymmetrically substituted pyrazole, which generally crystallizes exclusively as the most thermodynamically favoured prototropomer (Faure, Vincent, Rousseau, Claramunt & Elguero, 1988). We are aware of one other study where both possible tautomers were observed in a solid asymmetrically substituted N—H pyrazole, namely, 3{5}-(ferrocen-1-yl)pyrazole (Lopez, Claramunt, Trofimenko & Elguero, 1993); this result was derived from an NMR spectrum of an amorphous solid sample, however.

4. Spectroscopic studies

While several NMR criteria for the assignment of 3- and 5-substituted pyrazoles have been discussed (Elguero, 1984), the most generally applicable technique for the study of prototropomerism in these compounds is ^{13}C NMR spectroscopy (Lopez, Claramunt, Trofimenko & Elguero, 1993, and references therein). The two possible pyrazole tautomers (Fig. 1) can be distinguished on the basis of the chemical shift of the substituted (quaternary) C atom in the pyrazole ring, which appears at 146–152 p.p.m. when this is C(3), and at 137–141 p.p.m. when C(5); in the latter case, C(3) and C(5) generally resonate within 0–5 p.p.m. of each other. In addition, for 3{5}-aryl pyrazoles, the chemical shift of C(4) is dependent on the orientation of the aryl substituent relative to the pyrazole ring, this resonance being observed at 102–103 p.p.m. when these are coplanar or when there is free rotation about the linking C—C bond, and at 105–108 p.p.m. when the arene and pyrazole planes are sterically constrained to be twisted with respect to one another.

The solid-state ^{13}C NMR spectrum of crystalline (III) at room temperature clearly shows the presence of a single tautomer, with ten distinct peaks being observed which could be readily assigned by comparison with the solution spectrum of this compound in $CDCl_3$ (Table

6, Fig. 6*a*). Although, the resonances for C(3) and C(5) occur as a single broadened peak at δ = 140.3 p.p.m., the absence of a signal for C(5) in the range expected for tautomer *A* (Fig. 1) is consistent with the exclusive presence of the 5-substituted tautomer *B* in the crystal. By contrast, the ^{13}C NMR spectrum of solid (IV).1/2H_2O is complex, containing at least 14 distinct aromatic resonances (Fig. 6*b*), and is very similar to the solution spectrum of this compound obtained in $(CD_3)_2SO$ (Table 6). Using the rules described above, separate peaks in this spectrum can be assigned to tautomers *A* and *B* (Fig. 1), thus confirming the presence of prototropic disorder in this compound. The relative intensities of the two sets of peaks suggest that tautomer *B* has approximately twice the population of tautomer *A* in the crystal.

The ^{13}C NMR spectra of solid (III) and (IV).1/2H_2O between 293 and 370 K are sharp and in the slow exchange limit, suggesting that for both compounds the rate of interconversion of tautomers *A* and *B* in the crystal is slow (< 10^3 Hz) or that both structures are static. While the lack of fluxionality in the crystal for (III) can be ascribed to the intramolecular N—H···O hydrogen bond present in this compound, the static nature of the disorder present in (IV).1/2H_2O is harder to rationalize. However, an NMR study of 3,5-di(*tert*-butyl)pyrazole, which crystallizes as a cyclic dimer and exhibits disordered *tert*-butyl substituents, has shown that prototropomeric exchange in this compound is kinetically suppressed in those disorder orientations where the distribution of *tert*-butyl groups within the dimer is not symmetric and the proton transfer steps are non-degenerate (Aguilar-Parrilla *et al.*, 1995). Clearly, the proton transfers leading to exchange of the two disorder orientations in (IV).1/2H_2O (Fig. 5) are also non-degenerate, which may similarly suppress concerted proton transfer along the hydrogen-bonded chains in this compound.

The ^{1}H NMR spectrum of (III) in $CDCl_3$ and C_6D_6 at room temperature shows a broad resonance centred at 11.7 p.p.m. attributable to the N—H proton (Table 7), together with the seven other peaks expected for this molecule. The ^{13}C NMR spectrum of (III) in $CDCl_3$ is clearly consistent with the presence of purely a 5-substituted isomer and shows a C(4) resonance that suggests coplanarity between the pyrazole and arene rings (Table 6); a ^{13}C spectrum was not obtained in C_6D_6, because of the relatively low solubility of (III) in this solvent. By contrast, however, in $(CD_3)_2SO$ two distinct peaks for each of H(3)/H(5) and the N—H proton are observed by NMR, all integrating to approximately 0.5H (Table 7), which indicates the presence of both tautomeric forms (Fig. 1). The ^{13}C spectrum of (III) in this solvent shows two well separated peaks for each of C(3) and C(5) that can be clearly assigned to both tautomers *A* and *B* (Table 6). Interestingly, two peaks in the region expected for C(4) are also observed at

Table 6. *Selected solution (62.9 MHz) and solid-state (100.6 MHz) ^{13}C NMR data for (III) and (IV)*

Assignments of peaks to tautomers *A* or *B* (Fig. 1) have been made only where these are unambiguous.

	δ (p.p.m.)			
	C(3)	C(4)	C(5)	C(1′)
(III)				
$CDCl_3$	138.2*	103.3	141.2*	119.0
$(CD_3)_2SO$	147.2,† 138.8*	106.1, 105.3	129.3,† 139.6*	119.0, 123.7
Solid state	140.3‡	102.8	140.3‡	118.4
(IV)				
$CDCl_3$	–§	102.1	133.2 (br)	125.2
$(CD_3)_2SO$	150.5,† 140.3¶	101.6	129.8,† 141.9¶	127.1, 122.6
Solid state	153.0,† 141.0¶	103.1 (br)	130.5† 143.7¶	127.0, 123.2

*Tautomer *B* (Fig. 1). †Tautomer *A* (Fig. 1). ‡These two resonances appear as a single broad peak. §Not observed. ¶Tautomer *B* (Fig. 1); these peaks could not be reliably assigned to either C(3) or C(5).

chemical shifts implying both non-coplanarity between the pyrazole and the phenyl rings and restricted rotation about the C(3)/C(5)—C(1′) bond, which could reflect steric hindrance by the 2′-methoxy group. Hence, it appears that the intramolecular hydrogen bond exhibited by (III) in the crystal survives in chloroform and benzene, but is not maintained in DMSO solution, the pyrrolic proton presumably now forming hydrogen bonds to solvent molecules. In addition, the preference of (III) for the 5-substituted tautomer in the solid state and in non-coordinating solvents appears to be imposed by the intramolecular N—H···O hydrogen bond, since both the

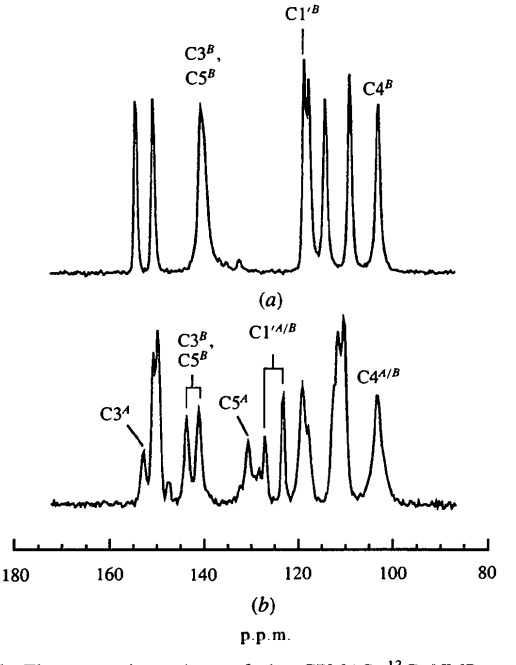

Fig. 6. The aromatic regions of the CPMAS ^{13}C NMR spectra (100.6 MHz, 293 K) of: (*a*) (III) (rotation frequency 8.2 kHz); (*b*) (IV).1/2H_2O (rotation frequency 8.6 kHz), with selected peak assignments. The superscripts *A* and *B* refer to the tautomers shown in Fig. 1.

Table 7. *Selected 250 MHz ^1H NMR data for (III) and (IV)*

	δ (p.p.m.) (*J*, Hz)		
	H(1)	H(3)/(5)	H(4)
(III)			
$CDCl_3$	11.7 (v. br)	7.61 (d, 1.9)	6.64 (d, 1.9)
C_6D_6	11.8 (v. br)	7.64 (br)	6.65 (br)
$(CD_3)_2SO$	13.02 (br)	7.76 (br)	6.77 (br)
	12.93 (br)	7.33 (br)	
(IV)			
$CDCl_3$	-*	7.55 (d, 2.2)	6.51 (d, 2.2)
C_6D_6	-*	7.50 (d, 2.2)	6.44 (d, 2.2)
$(CD_3)_2SO$	13.15 (br)	7.69 (v. br)	6.65 (br)
	12.81 (br)		

* Not observed.

3- and 5-substituted forms are similarly populated in conditions where this is not present.

For (IV) the pyrrolic proton H(1) is not observable by ^1H NMR in $CDCl_3$ or C_6D_6 at room temperature (Table 7); the ^{13}C NMR spectrum of (IV) in $CDCl_3$ is also inconclusive, since no peak assignable to C(3) could be observed while the C(5) resonance is extremely broadened (Table 6). As for (III), however, in $(CD_3)_2SO$ two distinct N—H ^1H resonances with a total integration of one proton are observed, in approximately a 2:3 ratio (Table 7); the H(3)/H(5) resonance is now considerably broadened, but is not split. The ^{13}C spectrum of (IV) in $(CD_3)_2SO$ again clearly shows the presence of both tautomers (Table 6), although this spectrum is too broadened to allow reliable determination of their relative populations. However, from these data it seems likely that the distribution of tautomers *A* and *B* for (IV).1/2H_2O is similar in the crystal and in DMSO solution (*vide supra*).

We thank the Royal Society (London) for a University Research Fellowship to MAH and the EPSRC for the diffractometer and solid-state NMR spectrometer.

References

Abboud, J.-L.M., Cabildo, P., Cañada, T., Catalán, J., Claramunt, R. M., de Paz, J. L. G., Elguero, J., Homan, H., Notario, R., Toiron, C. & Yranzo, G. I. (1992). *J. Org. Chem.* **57**, 3938–3946.

Aguilar-Parrilla, F., Cativiela, C., de Villegas, M. D. D., Elguero, J., Foces-Foces, C., Laureiro, J. I. G., Cano, F. H., Limbach, H.-H., Smith, J. A. S. & Toiron, C. (1992). *J. Chem. Soc. Perkin Trans. 2*, pp. 1737–1742.

Aguilar-Parrilla, F., Limbach, H.-H., Foces-Foces, C., Cano, F. H., Jagerovic, N. & Elguero, J. (1995). *J. Org. Chem.* **60**, 1965–1970.

Aguilar-Parrilla, F., Scherer, G., Limbach, H.-H., Foces-Foces, M. C., Cano, F. H., Smith, J. A. S., Toiron, C. & Elguero, J. (1992). *J. Am. Chem. Soc.* **114**, 9657–9659.

Bonati, F. (1989). *Gazz. Chim. Ital.* **119**, 291–300.

Catalán, J., Fabero, F., Claramunt, R. M., Santa Maria, M. D., Foces-Foces, M. C., Cano, F. H., Martínez-Ripoll, M., Elguero, J. & Sastre, R. (1992). *J. Am. Chem. Soc.* **114**, 5039–5048.

Cativiela, C., Laureiro, J. I. G., Elguero, J. & Elguero, E. (1991). *Gazz. Chim. Ital.* **121**, 477–481.

Elguero, J. (1984). *Comprehensive Heterocyclic Chemistry*, edited by A. R. Katritzky & C. W. Rees, Vol. 5, Ch. 4.04, pp. 182–197. Oxford: Pergamon Press.

Elguero, J., Cano, F. H., Foces-Foces, C., Llamas-Saiz, A. L., Limbach, H.-H., Aguilar-Parrilla, F., Claramunt, R. M. & López, C. (1994). *J. Heterocycl. Chem.* **31**, 695–700.

Faure, R., Vincent, E.-J., Rousseau, A., Claramunt, R. M. & Elguero, J. (1988). *Can. J. Chem.* **66**, 1141–1146.

Foces-Foces, C., Llamas-Saiz, A. L., Claramunt, R. M., López, C. & Elguero, J. (1994). *J. Chem. Soc. Chem. Commun.* pp. 1143–1145.

Halcrow, M. A., Cromhout, N. L., Powell, H. R. & Raithby, P. R. (1996). To be published.

Halcrow, M. A., Raithby, P. R. & Rennie, M.-A. (1996). To be published.

Lin, Y. & Lang, S. A. Jr (1977). *J. Heterocycl. Chem.* **14**, 345–347.

Llamas-Saiz, A. L., Foces-Foces, C., Cano, F. H., Jiménez, P., Laynez, J., Meutermans, W., Elguero, J., Limbach, H.-H. & Aguilar-Parrilla, F. (1994). *Acta Cryst.* B**50**, 746–762.

Llamas-Saiz, A. L., Foces-Foces, C. & Elguero, J. (1994). *J. Mol. Struct.* **319**, 231–260.

Llamas-Saiz, A. L., Foces-Foces, C., Elguero, J. & Meutermans, W. (1992). *Acta Cryst.* C**48**, 714–717.

Llamas-Saiz, A. L., Foces-Foces, C., Sobrados, I., Elguero, J. & Meutermans, W. (1993). *Acta Cryst.* C**49**, 724–729.

Lopez, C., Claramunt, R. M., Trofimenko, S. & Elguero, J. (1993). *Can. J. Chem.* **71**, 678–684.

Sheldrick, G. M. (1987). *SHELXTL-Plus*. PC Version. Siemens Analytical X-ray Instruments Inc., Madison, Wisconsin, USA.

Sheldrick, G. M. (1990). *Acta Cryst.* A**46**, 467–473.

Sheldrick, G. M. (1993). *SHELXL93. Program for the Refinement of Crystal Structures*. University of Göttingen, Germany.

Smith, J. A. S., Wehrle, B., Aguilar-Parrilla, F., Limbach, H.-H., Foces-Foces, M. C., Cano, F. H., Elguero, J., Baldy, A., Pierrot, M., Khurshid, M. M. T. & Larcombe-McDouall, J. B. (1989). *J. Am. Chem. Soc.* **111**, 7304–7312.